Development of a bioactive porous collagen/β-tricalcium phosphate bone graft assisting rapid vascularization for bone tissue engineering applications

Article *in* Journal of Biomedical Materials Research Part A · September 2017

DOI: 10.1002/jbm.a.36207

CITATIONS
18

READS
152

7 authors, including:

Mohammad Reza Nourani
Baqiyatallah University of Medical Sciences
125 PUBLICATIONS **1,218** CITATIONS
SEE PROFILE

Sm Javad Mortazavi
Tehran University of Medical Sciences
119 PUBLICATIONS **1,892** CITATIONS
SEE PROFILE

Fatemeh Bagheri
Royan Institute
38 PUBLICATIONS **315** CITATIONS
SEE PROFILE

Society For Biomaterials

Development of a bioactive porous collagen/β-tricalcium phosphate bone graft assisting rapid vascularization for bone tissue engineering applications

Nafiseh Baheiraei,[1] Mohamma Reza Nourani,[2] Seyed Mohammad Javad Mortazavi,[3] Mansoureh Movahedin,[1] Hossein Eyni,[1] Fatemeh Bagheri,[4] Mohammad Hadi Norahan[5]

[1]Department of Anatomical science, Faculty of Medical Sciences, Tarbiat Modares University, Tehran, Iran
[2]Chemical Injuries Research Center, Baqiyatallah University of Medical Sciences, Tehran, Iran
[3]Joint Reconstruction Research Center (JRRC), Tehran University of Medical Sciences, Tehran, Iran
[4]Department of Biotechnology, Faculty of Chemical Engineering, Tarbiat Modares University, Tehran, Iran
[5]Department of Biomedical Engineering, Islamic Azad University, Yazd Branch, Yazd, Iran

Received 21 January 2017; revised 17 August 2017; accepted 22 August 2017
Published online 26 September 2017 in Wiley Online Library (wileyonlinelibrary.com). DOI: 10.1002/jbm.a.36207

Abstract: We developed collagen (COL) and collagen/beta tricalcium phosphate (COL/β-TCP) scaffolds with a β-TCP/collagen weight ratio of 4 by freeze-drying. Mouse bone marrow-derived mesenchymal stem cells (BMMSCs) were cultured on these scaffolds for 14 days. Samples were characterized by physicochemical analyses and their biological properties such as cell viability and alkaline phosphatase (ALP) activity was, also, examined. Additionally, the vascularization potential of the prepared scaffolds was tested subcutaneously in Wistar rats. We observed a microporous structure with large porosity (~95–98%) and appropriate pore size (120–200 μm). The COL/β-TCP scaffolds had a much higher compressive modulus (970 ± 1.20 KPa) than pure COL (0.8 ± 1.82 KPa). *In vitro* model of apatite formation was established by immersing the composite scaffold in simulated body fluid for 7 days. An ALP assay revealed that porous COL/β-TCP can effectively activate the differentiation of BMMSCs into osteoblasts. The composite scaffolds also promoted vascularization with good integration with the surrounding tissue. Thus, introduction of β-TCP powder into the porous collagen matrix effectively improved the mechanical and biological properties of the collagen scaffolds, making them potential bone substitutes for enhanced bone regeneration in orthopedic and dental applications. © 2017 Wiley Periodicals, Inc. J Biomed Mater Res Part A: 106A: 73–85, 2018.

Key Words: angiogenesis, bone substitute, collagen, β-tricalcium phosphate, tissue engineering

How to cite this article: Baheiraei N, Nourani MR, Mortazavi SMJ, Movahedin M, Eyni H, Bagheri F, Norahan MH. 2018. Development of a bioactive porous collagen/β-tricalcium phosphate bone graft assisting rapid vascularization for bone tissue engineering applications. J Biomed Mater Res Part A 2018:106A:73–85.

INTRODUCTION

According to the American Academy of Orthopedic Surgeons (AAOS), 6.3 million bone fractures occur in the United States annually due to bone tumor removal, severe nonunion fractures, and traumatic accidents.[1,2] Bone defects are a fundamental public health issue, and are the leading cause of morbidity and disability in elderly patients.[3] After blood transfusion, bone is the second most commonly implanted material in the human body, with approximately 600,000 bone graft procedures performed annually.[4]

Although autografting (commonly from the iliac crest) is considered the gold standard in bone defect repair, it is limited by increased donor site morbidity, limited availability, and an invasive harvesting procedure. Allografting provides increased osteoconductive capacity while allowing for the use of large and differently shaped pieces of bone, but it also carries a high risk of potential infection, nonunion, fatigue fracture, and rejection.[3,5] Metallic- and ceramic-based artificial implants may provide immediate support at the defect site, but are limited by material-related failure modes such as poor integration with the surrounding tissue, corrosion failure, and brittleness/low tensile strength.[6]

Tissue engineering techniques provide a new method of regenerating damaged or diseased bone tissue. Scaffolds require materials with biocompatibility to protect against host immune rejection responses, osteoconduction ability for facilitating bone formation, suitable mechanical properties to ensure mechanical compatibility with the surrounding tissues, proper porous structure to provide enough space for cell proliferation and extracellular matrix (ECM) formation, and an adjustable rate of biodegradation matching the rate of tissue regeneration in the repaired area.[7,8]

Correspondence to: N. Baheiraei; e-mail: n.Baheiraei@modares.ac.ir
Contract grant sponsor: Iran National Science Foundation (INSF); contract grant number: 95822536

Several polymers and inorganic/organic biomaterials have been utilized as scaffolds for bone tissue engineering in recent years to meet the various demands that single-component scaffolds cannot.[9–14] Beta-tricalcium phosphate (β-TCP)/collagen (COL) is one of the best materials for fulfilling the requirements of bone tissue engineering scaffolds.[7] TCP replacements have been used as synthetic bone void fillers in dental and orthopedic applications for two decades because they are biocompatible and have high mechanical stiffness.[15,16] Among TCP substitute materials, β-TCP has a microstructure (Ca/P ratio) very close to that of natural bone tissue with good biodegradability and osteoconductivity.[17–20] It was one of the earliest calcium phosphate bone graft substitutes used by Albee and Morrison in 1920. An increased rate of bone union was reported when β-TCP was injected into the gap of a segmental bone defect.[21] This calcium phosphate ceramic has been widely used as an alternative to autografts in bone grafting,[22] and has excellent osteoconductivity and resorbability when used to fill bone defects.[23–30] Moreover, scaffolds based on calcium phosphate provide promising mechanical stability for implantation in load-bearing defects.[31] During bone regeneration, β-TCP exhibits resorbable characteristics and is completely replaced by new bone tissue after stimulation of bone formation.[32] The resorption rate of β-TCP is higher than that of highly crystalline sintered hydroxyapatite, which has an extremely slow resorption rate. Other calcium phosphate ceramics also have higher solubility than the rate of bone tissue regeneration, which makes them unsuitable for the gradual process of new bone tissue replacement.[33]

Collagen type I is a major component of the bone ECM; it has good biodegradability, excellent biological compatibility, and facilitates cell attachment,[34] resulting in better conditions for bone formation. However, it has inferior mechanical properties, specifically stiffness. Collagen has also demonstrated therapeutic promise in both preclinical and early clinical studies.[35] Therefore, incorporation of calcium phosphates with collagen results in the ideal biological scaffold, with materials similar to natural bone and the essential mechanical stiffness at different stages of bone regeneration.[36] β-TCP and collagen materials, especially when combined with concentrated bone marrow (BM) aspirate, provide an excellent substitute for bone, and offer an osteoconductive, osteoinductive, and osteogenic source for the formation of new bone.[37]

Zou et al. prepared a β-TCP/collagen composite with a bone-like microstructure that showed no cytotoxicity and resulted in complete bone tissue regeneration after 12 weeks *in vivo*.[7] Bulgin et al. combined β-TCP and absorbable atelocollagen with freshly isolated autologous BM-derived mononuclear cells to treat an aneurysmal bone cyst in a 10-year-old child. This treatment was used to fabricate a reasonable and beneficial substitute to promote bone cyst healing with both osteoinductive and osteoconductive features. The authors observed that β-TCP and freshly isolated cells had excellent handling characteristics and were well tolerated by the patient. They also detected significant clinical and radiographic improvements, with no adverse tissue reaction, infection, or delayed healing during the course of the treatment.[35] The authors of another study evaluated the effect of a prepared complex comprising β-TCP granules, collagen, and fibroblast growth factor-2 (FGF-2) on cortical bone repair in rabbits. The results suggested that bone formation is affected by resorption of β-TCP and may be promoted by FGF-2 in the β-TCP implantation site. The authors reported that the paste-like material was easy to handle in the treatment of cortical bone defects.[22]

In a typical bone tissue engineering approach, a bone graft is made using mesenchymal stem cells (MSCs) cultured in a porous scaffold for a certain length of time and then implanted into the defect.[38] It has been reported that osteochondral tissues may be effectively regenerated by integrating biodegradable scaffolds with MSCs.[39,40] Scaffolds comprising organic/inorganic composites such as collagen/β-TCP with MSCs are considered good candidates for bone tissue engineering.[8]

MSCs are multipotent and secrete many kinds of trophic and immunomodulatory cytokines with the ability to differentiate into multiple connective and bony tissues. They also play a role in various human tissue engineering applications, including treating non-unions and supporting healing in high-risk fusion procedures. The immunomodulatory characteristics of MSCs allow for the use of cells of allogeneic origin.[37]

In the present study, we fabricated porous COL and COL/β-TCP nanocomposite scaffolds by freeze-drying. Mouse bone marrow-derived mesenchymal stem cells (BMMSCs) were then cultured in these scaffolds for up to 14 days. Finally, we evaluated the physicochemical and biological characteristics of the samples, and investigated the vascularization and MSC differentiation associated with them.

MATERIALS AND METHODS

Synthesis of scaffolds

A porous COL/β-TCP composite was prepared as follows. First, collagen type I (CCS-1, NZA, Iran) was dispersed in dilute hydrochloric acid (pH = 2) at room temperature to produce a 1% (w/v) solution. A designated amount of β-TCP (Sigma-Aldrich) powder with a weight ratio of β-TCP/COL = 4/1 was then added to the collagen solution while stirring. After a homogeneous suspension had formed, we poured the mixture into a plastic mold and froze it at −20°C for 4 h and −80°C overnight. Subsequently, the frozen sample was further lyophilized to create a porous COL/β-TCP composite) freeze drier; ALPH1–2LD, UK). A similar protocol was used to make COL scaffolds without β-TCP. The obtained scaffolds were crosslinked for 24 h with 0.5% glutaraldehyde solution (GA; Merck, Germany). Porous samples were then soaked in deionized water for 4 days, refreshing daily to remove remnants of the GA. The samples were lyophilized again to form the scaffolds for subsequent experiments.

Bone marrow MSC isolation and expansion

BM was collected from the femurs and tibiae of 6–8-week-old mice that had been sacrificed by cervical dislocation.

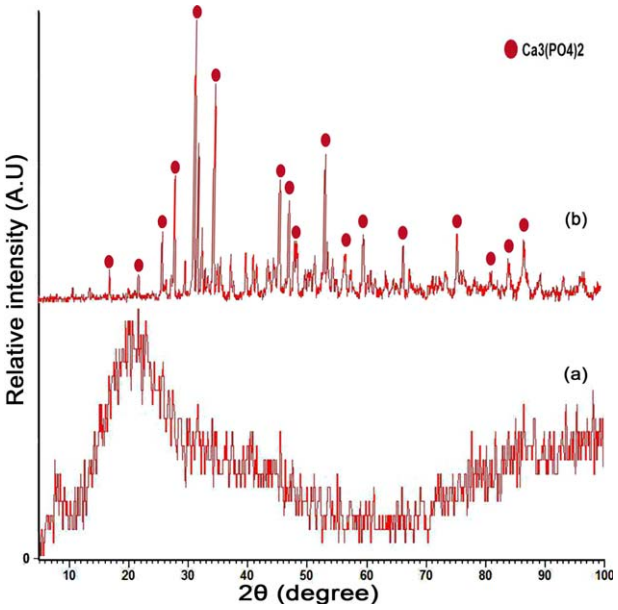

FIGURE 1. XRD patterns of (a) COL and (b) β-TCP/COL scaffolds.

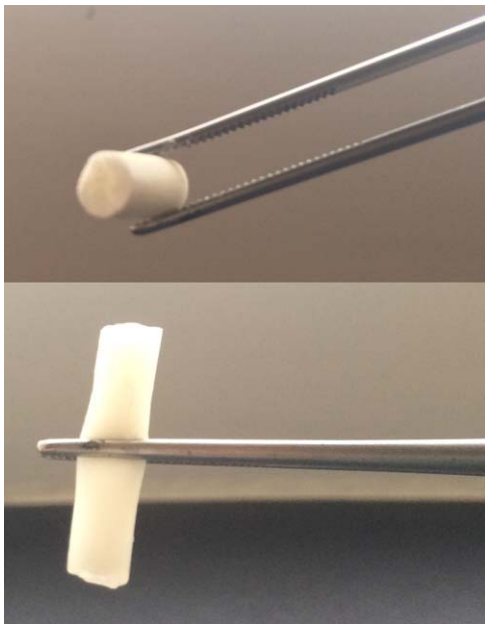

FIGURE 3. Optical micrographs of β-TCP/COL scaffold.

The animal experiments were approved by the Ethics Committee of Tarbiat Modares University, Iran (IR.TMU.REC.1395.388). The femurs and tibiae were carefully cleaned of adherent soft tissue, and the BM was harvested by flushing with Dulbecco's Modified Eagle's Medium (DMEM; Gibco, Germany) containing 100 IU/mL penicillin, 100 IU/mL streptomycin, and 15% fetal bovine serum (FBS; Gibco, Germany). After centrifugation for 5 min, the BM was mixed with the medium and incubated at 37°C in 5% CO_2. Forty-eight hours later, non-adherent cells were removed by medium replacement. We then incubated the cultures until they reached confluence, replacing the medium twice per week, and used passage-3 cells for subsequent experiments.

Characterization

Scaffold analyses. To analyze the crystalline phase of the scaffold powder, X-ray diffraction (XRD) was performed using a diffractometer with a Cu anode (D5000; Siemens) at a fixed incident angle of 0.02 in a 2θ range of 5–100°. After gold coating, the morphology of the prepared samples was examined by scanning electron microscopy (SEM; XL30, Philips). The scaffolds were quenched in liquid nitrogen and broken into pieces for the cross-sectional study. The macroscopic morphology of the prepared scaffolds was examined using an optical microscope (Olympus, GX51). Fourier transform infrared spectroscopy (FTIR; PE1760x) was performed in the range 500–4000 cm^{-1} at a scan speed of 23 scans/min with a resolution of 1 cm^{-1} in KBr-diluted medium to investigate the interaction between β-TCP particles and collagen fibrils. Transmission electron microscopy (TEM; Zeiss-EM10C) was used to characterize the precipitate particles within the collagen matrix. Samples were fixed and embedded in resin, then thin-sectioned by ultramicrotomy. The sections (50- to 70-nm thick) were collected on a copper mesh grid for subsequent experiments.

The porosity of the prepared scaffolds was measured by liquid displacement according to the following formula; the samples were cut to 2 × 1 × 0.5 cm^3, and ethanol was used as a liquid medium.[3]

$$\text{Porosity } (\%) = (W_2 - W_3 - W_S)/(W_1 - W_3) \times 100 \qquad (1)$$

where W_1 is the weight of the bottle filled with ethanol; W_2 is the weight of the bottle filled with ethanol after immersion of the scaffold; W_3 is the weight of the bottle filled with ethanol after removal of the scaffold; and W_s is the weight of the dry scaffold in air.

The bioactivity of the COL/β-TCP scaffold was evaluated *in vitro* from samples immersed in simulated body fluid (SBF) at 37°C for 3 and 7 days. The scaffolds were removed from the SBF, washed with deionized water, and dried. The morphology and Ca/P ratio of the created crystals on the scaffold surface were evaluated using a SEM equipped with an energy-dispersive X-ray analyzer (EDX; Rontec).

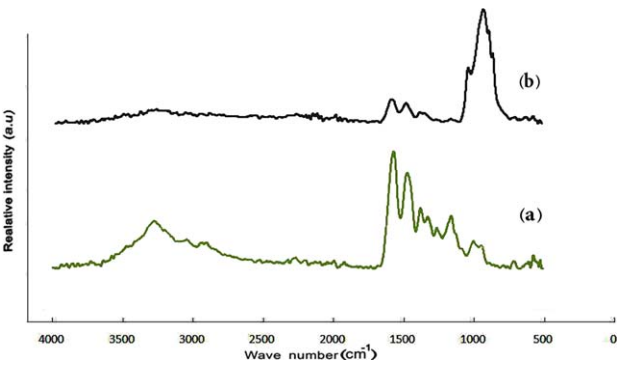

FIGURE 2. FTIR spectra of (a) COL and (b) β-TCP/COL scaffolds.

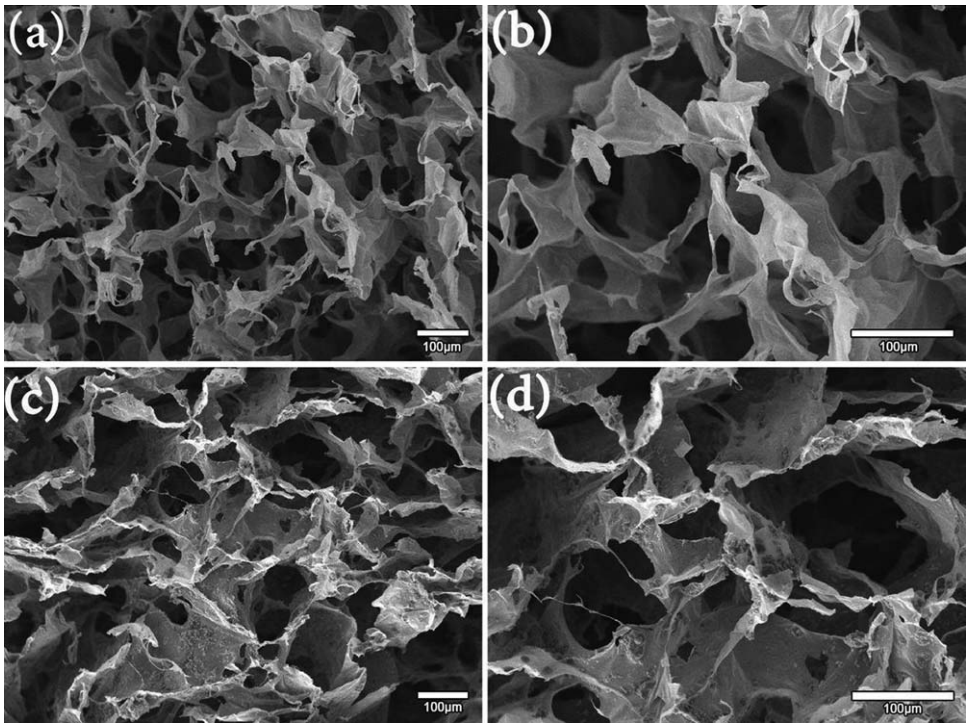

FIGURE 4. SEM images of surface morphology of the prepared scaffolds with different magnifications; (a), (b) COL and (c), (d) β-TCP/COL scaffolds.

The compressive strength of the scaffolds was determined using a conventional testing machine (H10KS; Hounsfield) at a loading rate of 1 mm/min. The compressive modulus was calculated from the slope of the stress–strain curve in the linear region. Three specimens were tested from each scaffold.

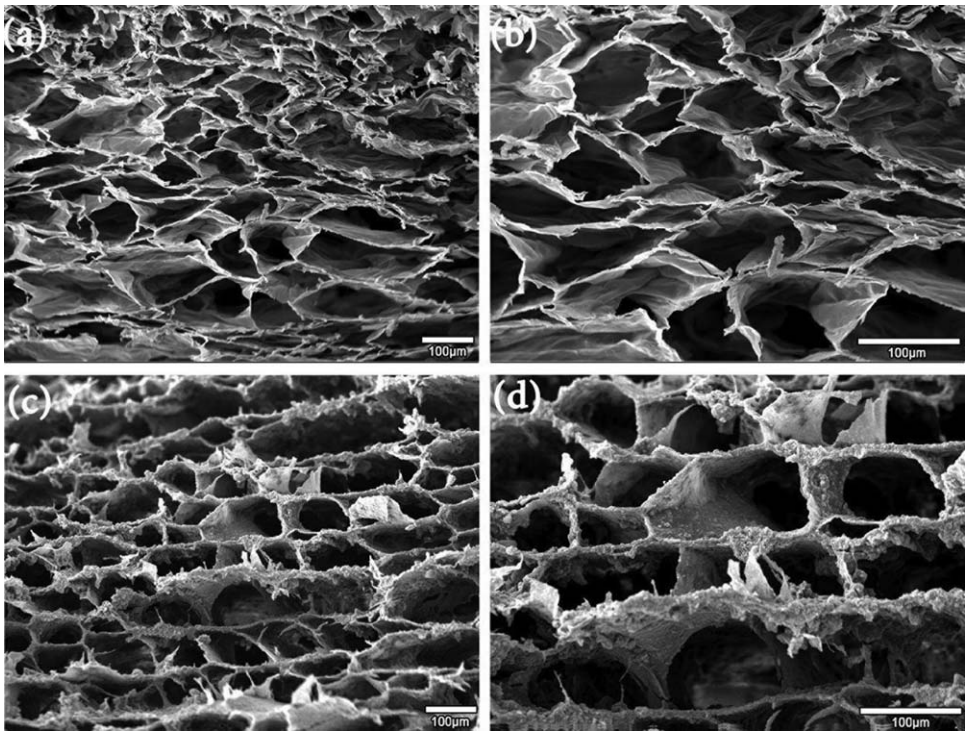

FIGURE 5. SEM images of the cross section of the prepared scaffolds with different magnifications; (a), (b) COL and (c), (d) β-TCP/COL scaffolds.

TABLE I. Characterizations of COL and β-TCP/COL Scaffolds

Scaffolds	Pore Size (μm)	Porosity (%)	Compressive Modulus (KPa)
COL	150–200	98.4 ± 1.29	0.8 ± 1.82
COL/β-TCP	120–150	95.5 ± 1.78	970 ± 1.20

The swelling ratio was used to quantitatively evaluate the swelling behavior of each scaffold.[8] The scaffolds were placed in phosphate-buffered saline (PBS; Gibco, Germany, pH = 7.4) at 37°C in a humidified atmosphere of 5% CO_2 for 1, 3, 24, and 48 h. At each time-point, the samples were taken out, and the excess PBS was removed by blotting on filter article. The swelling ratio was quantified using the following formula[41]:

$$\text{Swelling ratio} = (W_{\text{wet}} - W_{\text{dry}})/W_{\text{dry}} \quad (2)$$

where W_{dry} is the weight of the dry scaffold and W_{wet} is the weight of the scaffold immersed in PBS.

To assess the hydrolytic degradation of the synthesized scaffolds, sterilized and carefully dried samples were weighed and placed in PBS (pH = 7.4) in a water bath (Memmert, WB14) at 37°C. At different intervals, samples were removed, washed with deionized water, and completely dried in a vacuum. The weight loss percentage was calculated as:

$$\text{Weight loss}\ (\%) = (W_1 - W_2)/W_1 \times 100 \quad (3)$$

where W_1 and W_2 are the weights of the scaffolds before and after degradation, respectively.[42] We recorded the average value from three different samples.

Cytotoxicity and morphology assessments. The scaffolds were sterilized using 70% ethanol and washed with PBS. Then, 10^4 cells were suspended in expansion medium, seeded over scaffolds in 96-well culture plates, and incubated in a humidified chamber at 37°C in 5% CO_2. A cytocompatibility assessment was performed using 3-[4,5-dimethylthiazol-2-yl]-2,5-diphenyltetrazolium bromide (MTT, Sigma) colorimetric assay at 48 and 96 h. Briefly, the scaffolds were washed with PBS, a 150 μL solution containing a 5:1 ratio of media and MTT (5 mg/mL in PBS) was added to each well, and the scaffolds/cells were incubated. Two-hours later, the medium was removed, and the formazan precipitates were dissolved in dimethyl sulfoxide (DMSO). The optical absorbance at 570 nm was measured using a microplate reader (ELISA reader, ELX808, BioTek). At least three samples were averaged for each experiment. The cells on the tissue culture plate (TCP) were considered the control. Cell viability was calculated as a percent value relative to the control group. To evaluate the possible cytotoxicity of the released degradation products, cross-linked samples were immersed in the culture medium and incubated at 37°C in 5% CO_2 for 10 days. After incubation, the samples were removed and the extracts were used for indirect cytotoxicity analysis. Briefly, 1×10^4 cells/well were plated onto 96-well plates and incubated at 37°C for 24 h in a humidified atmosphere of 5% CO_2. The medium was then replaced by the extract obtained after 10 days, and the cells were incubated for a further 24 h before performing the MTT assay. The control group was given the normal medium.

The morphology of the cultured cells in the prepared samples was assessed by SEM. After 48 h, the attached cells were fixed in 2.5% glutaraldehyde followed by serial dehydration with graded ethanol solutions (10, 30, 70, 90, and 100%), coated with gold, and examined at an accelerating voltage by SEM (XL30; Philips).

Alkaline phosphatase activity. Alkaline phosphatase (ALP) activity was measured to quantitatively assess the osteogenic differentiation of the MSCs. The cells on the constructs were washed with PBS (pH 7.4), homogenized with 1 mL

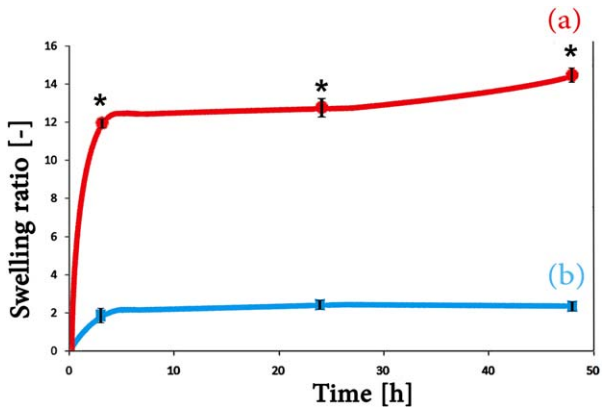

FIGURE 6. Water uptake of the (a) COL and (b) β-TCP/COL scaffolds at different time points. The result is presented as the means ± standard deviation for $n = 3$. * indicates $p < 0.01$ versus β-TCP/COL scaffold at each day.

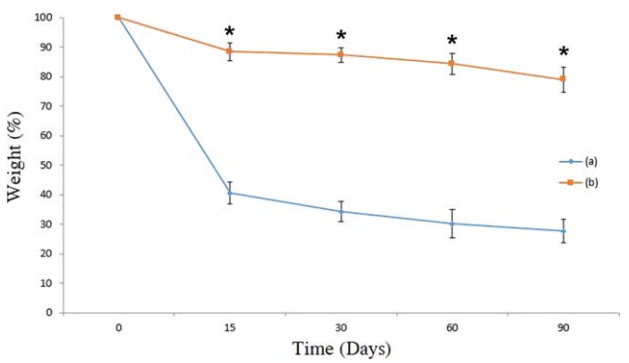

FIGURE 7. Weight loss of (a) COL and (b) β-TCP/COL scaffolds in PBS (pH 7.4). The result is presented as the means ± standard deviation for $n = 3$. * indicates $p < 0.01$ versus COL scaffold at each day.

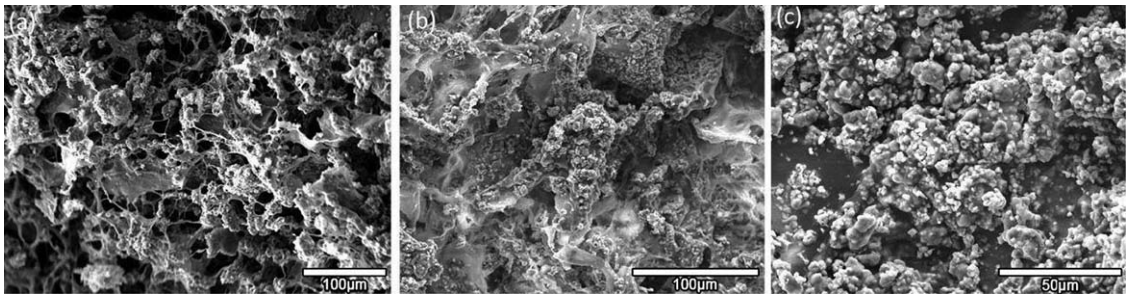

FIGURE 8. SEM micrograph of the scaffolds immersed in SBF after (a) 3 day and (b), (c) 7 days.

PBS, and sonicated. The cell lysate (0.1 mL) was mixed with 0.2 mL of *p*-nitrophenyl phosphate (pNPP) substrate solution (BioVision). After incubation at 37°C for 30 min, 2*M* NaOH solution was added to stop the reaction.[43] Absorption at 405 nm was read using a microplate reader (Stat Fax 3200; Awareness Technology).

Subcutaneous implantation, and histological and immunohistochemical analyses. To evaluate the *in vivo* angiogenic properties of the scaffolds, subcutaneous implantation was performed. Eighteen male NMRI mice (25–30 g, age = 6–8 weeks) were used. Three days prior to transplantation, animals received cyclosporine (Novartis Pharma AG, Switzerland) with their drinking water.[44] General anesthesia was induced by intraperitoneal injection of a mixture of ketamine (Alfasan, The Netherlands; 0.04 mL/100 g body weight) and xylazine (Alfasan, The Netherlands; 0.02 mL/10 g body weight). A small transverse incision (approximately 2-cm long) was made on the backs of the mice, and 10 × 10 mm^2 scaffolds were subcutaneously implanted (group 1: COL; group 2: composite (COL/β-TCP), $n = 3$ per group). The incision was then closed with a surgical suture. The mice recovered from the surgery, were permitted free access to food and water, and all survived without any complications. They were then sacrificed after 1, 2, and 4 weeks. Local vascularization around and inside the scaffolds was examined under a stereo microscope (SMZ 1000, Japan). The implantation bed was explanted with the surrounding tissue, fixed in 10% buffered formalin for 24 h, and transferred to PBS at 4°C. Fixed tissues were cut into several segments of 5-μm thickness and stained with Mayer's hematoxylin and eosin (H&E) to assess cellularization. Images were taken with an AxioCam camera on an AxioPlan microscope (Carl Zeiss GmbH, DE). The cell migration rate was calculated as follows:

$$\text{Cell migration rate} = (W/W_0)\ \% \qquad (4)$$

where W is the cell migration area into the scaffold and W_0 is the area of the scaffold.[36]

Immunohistochemistry assessments were also performed to visualize vascularization. The samples were embedded in paraffin, dewaxed, and blocked with 3% (w/v) bovine serum albumin in PBS (pH 7.4) for 20 min at 20°C. The sections were incubated for 12 h at 4°C with the primary antibody of anti-VEGFR2 (1:100; Abcam), and washed three times with PBS for 5 min each time. Coloration was achieved using a staining kit containing a peroxidase-conjugated polymer that carried antibodies to rabbit and mouse immunoglobulins. Positive cells were revealed using diaminobenzidine (DAB) chromogen (Vector Laboratories, Burlingame). Counterstaining was carried out with hematoxylin and the slides were dehydrated and mounted. The slides were examined using a light microscope, and the mean blood vessel number was determined. At least four sections of each scaffold and six images per section were investigated to obtain the data.

Statistical analysis

Values are expressed as means ± standard deviations (SDs). The data were analyzed by one-way analysis of variance (ANOVA) using SPSS 16.0 software (SPSS). *P*-values of < 0.05 were considered significant.

RESULTS AND DISCUSSION

Although collagen scaffolds exhibit excellent biological performance, they do not have adequate mechanical properties for implantation into load-bearing defects, which limits their potential use in bone tissue engineering. However, a composite of β-TCP/COL is one of the best materials for meeting the essential criteria for bone tissue engineering.[7] In this study, β-TCP particles were added to acidic disassembled collagen to evaluate the effect of the particles on the

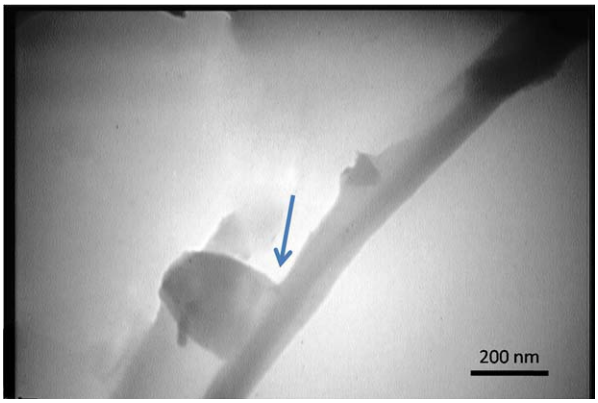

FIGURE 9. TEM micrograph of β-TCP/COL scaffolds. Arrow indicates tight contact between β –TCP particles and collagen.

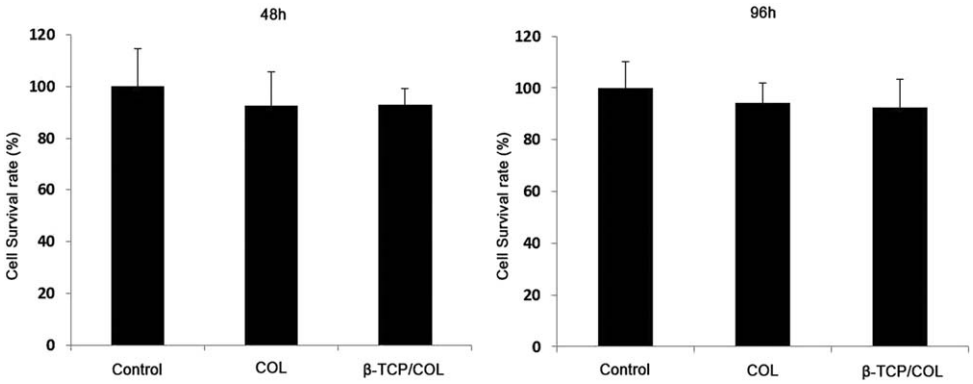

FIGURE 10. MTT assay results of COL and β -TCP/COL composite. Cell viability was calculated as percent value relative to the control group. Data were shown as mean ± SD from three independent experiments.

physicochemical and biological characteristics of the collagen scaffold.

Collagen fibrils are made of polypeptide chains connected by intermolecular covalent and hydrogen bonds.[45] The carboxylic groups of the disassembled fibrils are able to react with other species in the solution, including β-TCP particles. The dissolution reaction of β-TCP particles is pH-dependent, and an acidic medium (pH = 2) results in chemical bonding of the Ca ions of the particles and the carboxyl groups of the polypeptide chains of collagen, ensuring β-TCP integration with collagen.

The XRD patterns of pure collagen and the β-TCP/COL composite are shown in Figure 1. According to the Joint Committee on Powder Diffraction Standards (JCPDS; Card NO.70–2065), the resulting composite retains the $Ca_3(PO4)_2$ phase without other Ca phosphates. However, owing to its amorphous structure, the collagen scaffold did not exhibit peaks in the XRD pattern.

The chemical structure of the prepared scaffolds was confirmed by FTIR spectroscopy (Fig. 2). The FTIR spectrum of the collagen scaffold exhibited peaks at 1236, 1542, 1643, 3063, and 3295 cm^{-1} attributable to the amide III, II, I, B, and A functional groups, respectively.[46] For the composite scaffold, peaks observed at 660 and 1008 cm^{-1} were attributable to the PO_4^{-3} of β-TCP, and those at 1547 and 1650 cm^{-1} were due to the functional groups of the collagen.[13]

The composite scaffold shown in Figure 3 has a white spongy macroscopic appearance. The SEM images of both scaffolds with their cross-sectional morphology are illustrated in Figures 4 and 5. As shown, the β-TCP particles were homogenously distributed in the pore walls. The cross-sectional images show ordered collagen fibrils containing adherent β-TCP particles. The pores in both scaffolds were interconnected. This interconnected structure is beneficial for cell proliferation, migration, and nutritive transportation in bone tissue engineering.[47] The porous composite and collagen had high porosity with appropriate pore sizes of approximately 120–150 μm and 150–200 μm, respectively (Table I). Owing to the added β-TCP, the scaffolds had a rougher surface with slightly reduced porosity and decreased pore size, as has been reported previously.[8,36]

The swelling ratio of a scaffold plays an important role in tissue culture, and affects cell growth and differentiation.[47] The swelling behavior is shown in Figure 6. Collagen swelling increased rapidly to 11.91 ± 0.05 within 3 h, and then continued increasing gradually to approximately 14.33 ± 0.08 before reaching a plateau. The composite scaffolds reached their maximum of approximately 1.86 ± 0.08 after 3 h, followed by another increase to 2.38 ± 0.05, and then they remained steady. The collagen scaffold had a much higher swelling ratio than the composite scaffold($p < 0.01$). The swelling capacity of the composite depends on the collagen and β-TCP content as well as the cross-linking density.[47] The deformability of the collagen scaffold can increase the amount of PBS absorbed. Therefore, this scaffold was structurally instable with a much higher swelling ratio than the composite, which remained more stable because of the addition of β-TCP particles. The distribution of β-TCP powders in the collagen matrix of the composite can improve the structural stability of the composite scaffold.[8] The water uptake results revealed that both scaffolds reached the equilibrium swelling point in < 48 h, which is consistent with previous studies.[8,47]

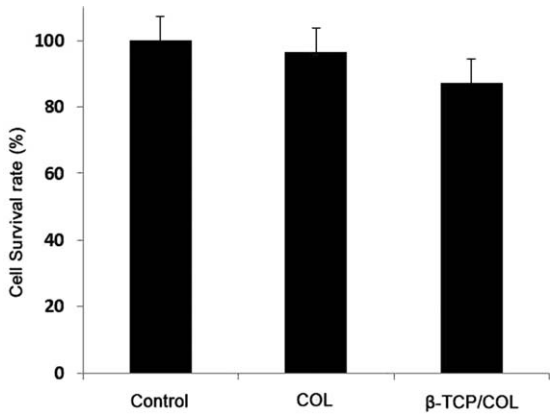

FIGURE 11. Effect of scaffolds extract on MSCs viability. Cell viability was shown as percent value relative to the control group. Data were shown as mean ± SD from three independent experiments.

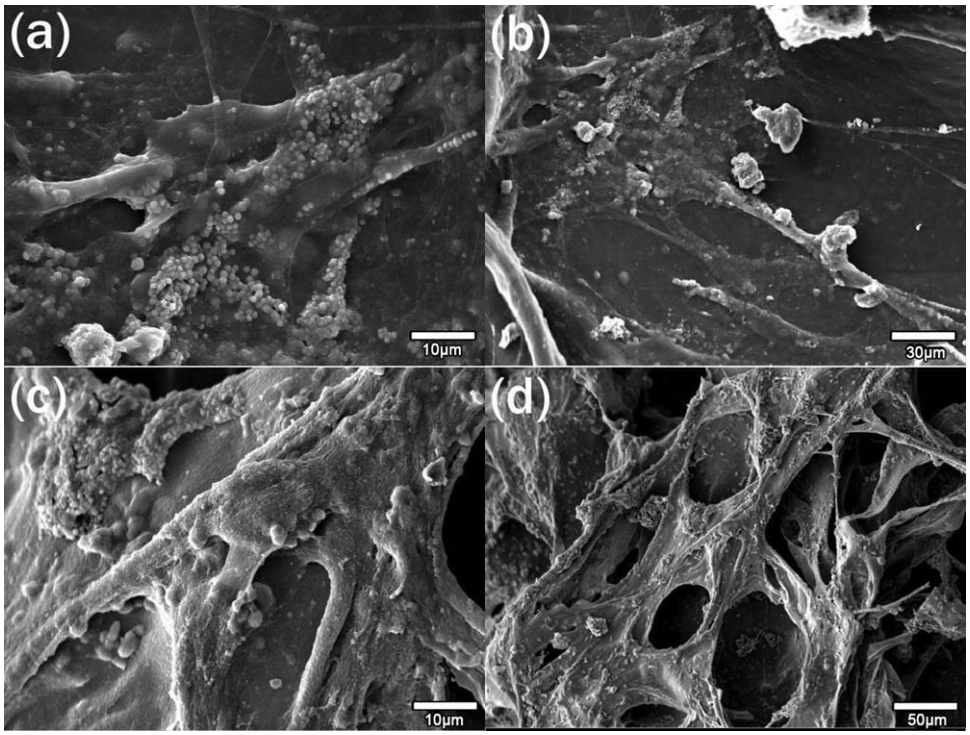

FIGURE 12. SEM photographs of MSCs cultured on (a), (b): COL scaffold and (c), (d) β-TCP/COL after 48 h. Cells spread relatively confluent on the surface of the scaffolds.

The quantitative weight loss data for both scaffolds are shown in Figure 7. As shown, the samples exhibited progressive mass loss over 90 days. Both scaffolds experienced rapid weight loss within 15 days. However, the figure was much higher for the COL sample ($p < 0.01$), which lost more than half its total weight (almost $60\% \pm 0.08$). This sample reached $27\% \pm 0.04$ of the primary weight during the incubation period. For scaffolds containing β-TCP, the speed of degradation was much slower, with a reduction of only approximately $30\% \pm 0.03$ over a 90-day period. Therefore, the β-TCP particles increased the integrity of the composite structure, hindering rapid degradation during the observed period. The results correspond to the slower swelling ratio observed for the composite scaffold.

Apatite formation on scaffolds immersed in SBF is often used to predict their bone-forming potential *in vivo*.[6] The immersion of the β-TCP/COL scaffold in SBF resulted in morphological changes on the surface of the scaffold (Fig. 8). EDX analysis showed that the major elements consisted of C, O, P, N, and Ca. The Ca/P atomic ratio was found to be 1.63 after 7 days, which is similar to the stoichiometric ratio of hydroxyapatite (data not shown).

A uniform microenvironment within the composite can be obtained when the β-TCP particles are fine, are distributed well within the composite, and are firmly bonded to the collagen fibrils.[7] The TEM micrograph in Figure 9 shows no voids between the collagen fibrils and the β-TCP particles, confirming strong bonding. The joint marked by the arrow shows no obvious interface, with a smooth transition from the collagen fibril to the β-TCP particle, as reported previously.[7] This shows that a chemical reaction occurred between the particles and the carboxyl groups in the polypeptide chains of the collagen.[48–51] This result was also confirmed by the FTIR spectra (Fig. 2). It has been reported that the bonding between β-TCP particles and collagen fibrils, and the distribution of the particles in the composite, depends strongly on the acidity of the collagen suspension. At a pH value of 2, these particles were dispersed and bonded well to the collagen fibrils, and as the pH increased the distribution deteriorated. Our results at pH 2 were also in line with a previous study showing well-distributed β-

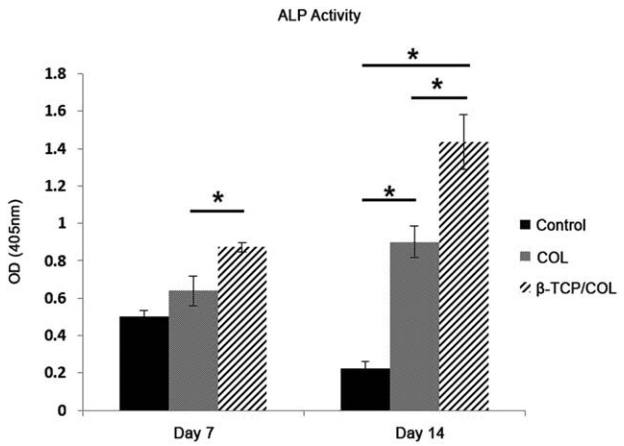

FIGURE 13. Comparison of the ALP activity for the cells in different groups after 7 and 14 days; This activity significantly increased in the cells cultivated on β-TCP/COL compared to others group. * indicates a statistically significant difference ($p < 0.05$).

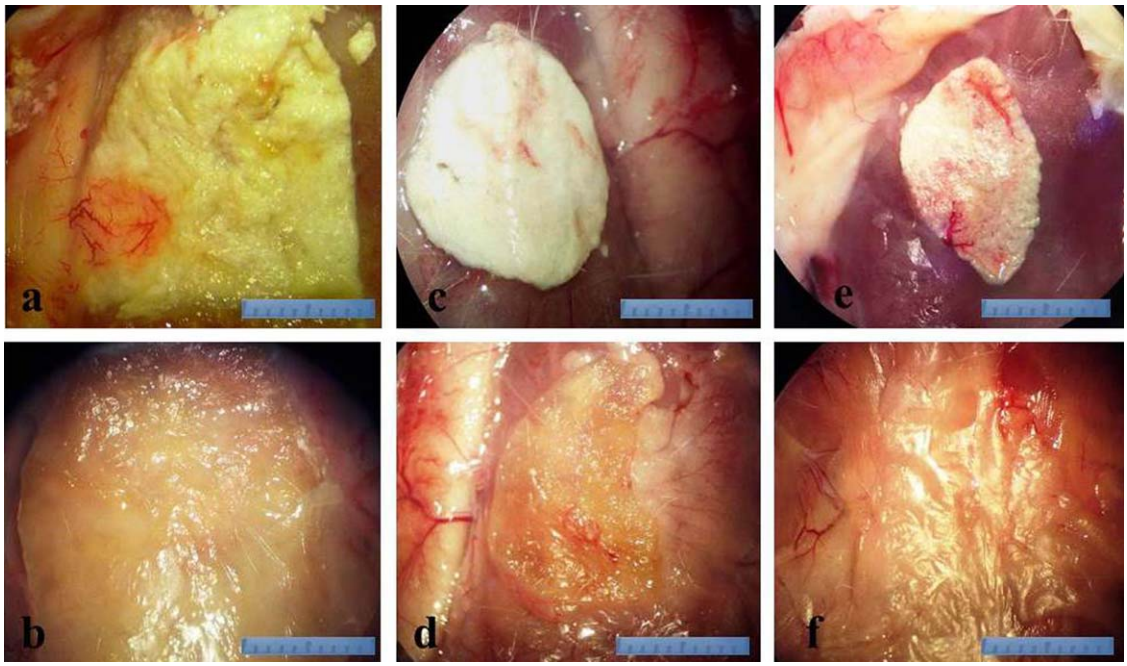

FIGURE 14. Gross morphology of the scaffolds after 1 (a, b), 2 (c, d) and 4 (e, f) weeks subcutaneous implantation; COL/β-TCP (a, c and e), COL (b, d and f). Scale bar: 10 mm.

TCP particles with round morphology within the collagen matrix.[7]

Appropriate mechanical properties are necessary for bone tissue engineering, especially for implanting constructs into load-bearing areas. The mechanical performance of the scaffolds was assessed by applying compression tests. Table I presents a summary of the mechanical properties of the prepared samples. As shown, the compressive modulus of the composite scaffold was much higher than that of the collagen scaffold ($p < 0.05$). This was due to the presence of β-TCP within the collagen matrix, which enhances the elastic modulus under compression.[47]

Cell viability was quantified by the MTT assay after culturing for up to 96 h (Fig. 10). As shown, there were no significant differences in cell viability between the scaffolds and the control. The 10-day extracts from the collagen and composite were also compared with the culture medium. The number of viable cells was slightly reduced in the composite group compared with the control group, but this difference was not significant (Fig. 11).

Cell morphology was investigated by SEM after 48 h. As shown in Figure 12, the cells expanded on the surfaces of both scaffolds. However, the surface of the composite was fully covered by proliferated cells, and the attached cells were spread and flattened on the surface. This confirms the high affinity of the cells for the surface of this scaffold.

The functional activity of the BMMSCs on the prepared scaffolds was assessed by measuring the ALP expressed by the cells after culturing for up to 14 days. The secretion of ALP was determined by pNPP assay at Days 7 and 14 (Fig. 13). Comparison of the ALP activity revealed that the combination of β-TCP and collagen (COL/β-TCP scaffold) can enhance and promote the differentiation of MSCs into osteoblasts significantly more than collagen. Furthermore, the cells cultured on collagen produced more ALP than those on TCP ($p < 0.05$).

β-TCP can create a desirable environment for the proliferation and differentiation of MSCs by providing a high concentration of calcium and phosphate ions (Ca^{2+} and PO_4^{-3} released in the culture medium), an adhesive surface morphology, and nucleation sites for apatite crystals. Such factors are thought to promote the osteogenicity of the MSCs.[49,52] For example, Arahira and Todo fabricated collagen/TCP composite scaffolds by the solid–liquid phase separation technique with subsequent freeze-drying. The MSCs were then cultured on prepared samples for up to 28 days. ALP activity was higher in the composite scaffold, with more active generation of osteoblastic markers than in the collagen sample. The authors stated that β-TCP can activate the differentiation of MSCs into osteoblasts and promote ECM formation. Structural stability is also considered an important factor affecting cell activity. It is assumed that cell proliferation inside the collagen scaffold is suppressed because of the shrinkage and deformation of the porous structure caused by swelling.[8]

In the present study, we assessed *in vivo* angiogenesis by retrieving the subcutaneous vascular scaffolds after 1, 2, and 4 weeks. Although both scaffolds maintained their well-defined morphology after 4 weeks, the COLL sample showed some degree of deformation with fewer vessel-sprouting structures (Fig. 14). As illustrated in Figure 15, the H&E images showed increased perivascular localization: both scaffolds were cellularized after 4 weeks. However, the cell migration rate for the COL/β-TCP scaffold significantly

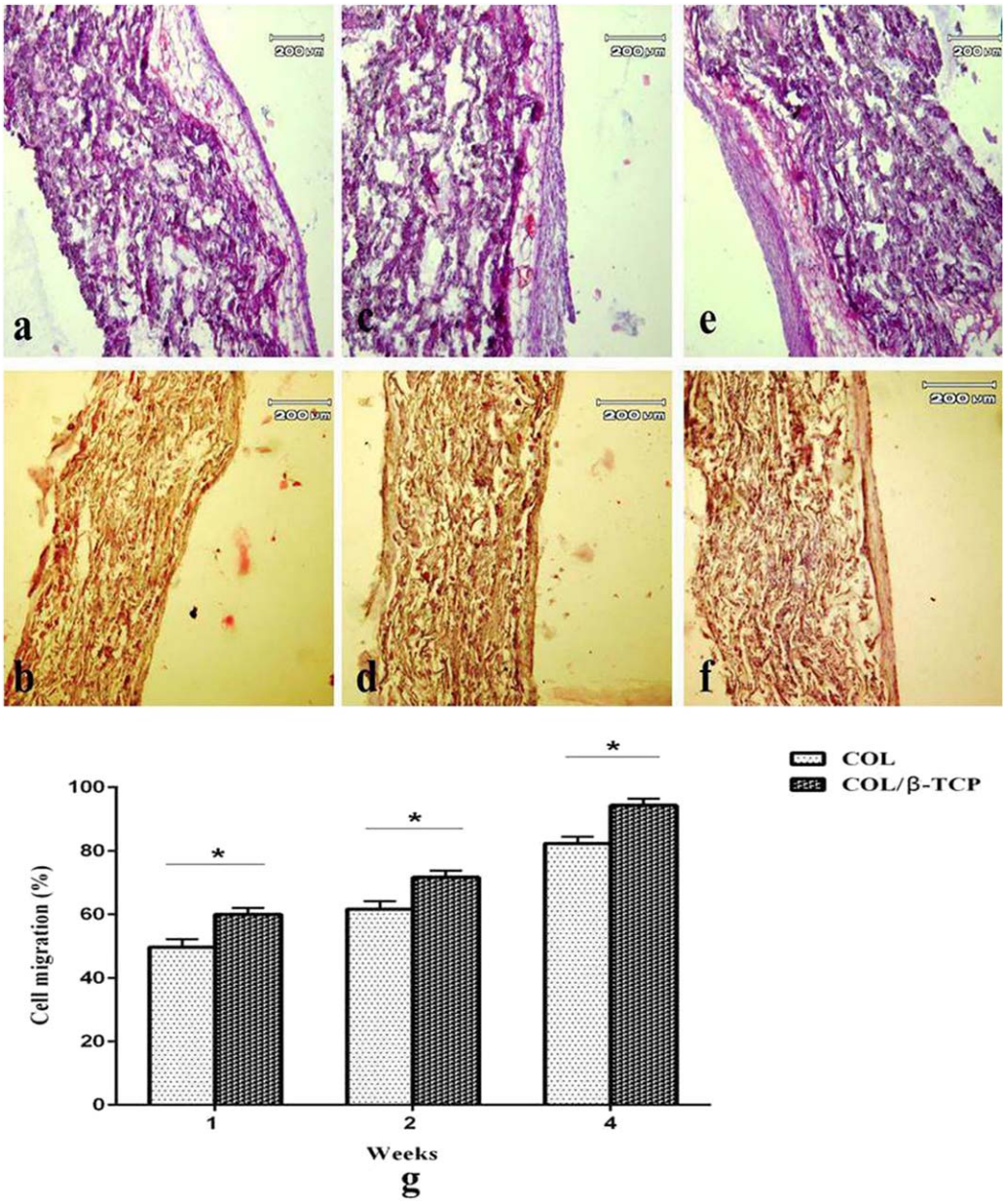

FIGURE 15. H & E staining of the scaffolds after 1 (a, b), 2 (c, d) and 4 (e, f) weeks subcutaneous implantation; COL/β-TCP (a, c and e), COL (b, d and f). Quantitative analysis of cell migration (g). * indicates a statistically significant difference ($p < 0.05$).

exceeded that of the COLL sample during the whole evaluation period, reaching approximately 90% after 4 weeks. Vascularization requires rapid and sufficient cellularization.[53] In this study, the composite scaffold provided a favorable environment for cell infiltration and migration. This resulted from the use of an appropriate composition and a scaffold with a suitable pore size.

Immunofluorescent staining with VEGFR2 was used to investigate the newly formed blood vessels in the cellularized area, which were further quantified based on the obtained images. More capillaries were identified on the composite scaffold, which corroborated the *in vitro* cell proliferation and differentiation results. Moreover, the COL/β-TCP scaffold promoted vascularization, and the quantitative results further confirmed that this scaffold significantly enhanced vessel density compared with COLL after 4 weeks (Fig. 16). The COL/β-TCP scaffold can help promote the efficient and rapid formation of a functional blood vasculature, which could benefit tissue engineering.[54]

To mimic the natural organic–inorganic ECM of the native bone, incorporation of calcium phosphate into polymer matrices has become a promising method of producing scaffolds for bone tissue engineering.[6] An osteoinductive calcium phosphate phase with a suitable porous collagen matrix can improve the material and biological properties of the obtained composite. Our results confirm the potential of

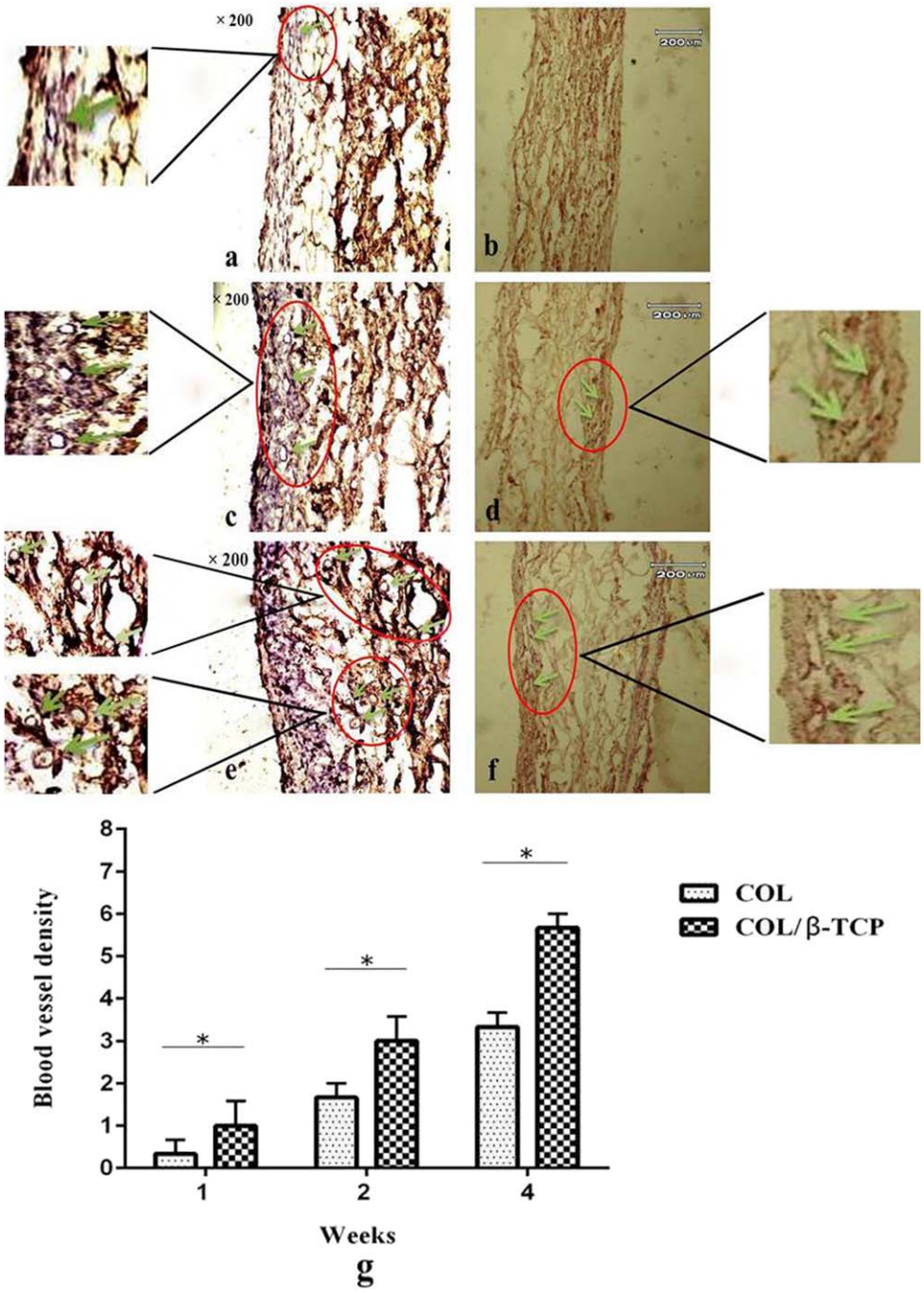

FIGURE 16. Morphological and Immunohistological analysis of microvasculature development in scaffolds stained with anti-VEGFR2 after 1 (a, b), 2 (c, d) and 4 (e, f) weeks subcutaneous implantation; COL/β-TCP (a, c and e), COL (b, d and f). The corresponding quantitative analysis on the density of blood vessel in the explanted scaffolds after 2 and 4 week subcutaneous implantation(g). * indicates a statistically significant difference ($p < 0.05$).

a β-TCP/COL scaffold to enhance bone regeneration and promote vascularization when used as a bone substitute in orthopedic and dental applications.

CONCLUSION

We successfully fabricated COLL and COL/β-TCP scaffolds with an interconnected pore structure. The composite showed that the β-TCP particles were homogenously distributed within the collagen matrix and had superior mechanical properties and ease of handling. This study clearly demonstrated the effectiveness of embedding β-TCP into the structure of the scaffold to promote the differentiation of BM MSCs into osteoblasts and further enhance ECM formation, as illustrated by the higher ALP activity and structural stability of the composite scaffold. More importantly, *in vivo*

subcutaneous vascularization was effectively enhanced in the COL/β-TCP scaffolds compared with their COL counterpart. The prepared composite has the potential for use as a bone substitute to enhance bone regeneration in orthopedic and dental applications.

CONFLICT OF INTEREST

The authors declare no conflict of interest.

REFERENCES

1. Stevens B, Yang Y, Mohandas A, Stucker B, Nguyen KT. A review of materials, fabrication methods, and strategies used to enhance bone regeneration in engineered bone tissues. J Biomed Mater Res B Appl Biomater 2008;85:573–582.
2. Greenwald AS, Boden SD, Goldberg VM, Khan Y, Laurencin CT, Rosier RN; American Academy of Orthopaedic Surgeons; The Committee on Biological Implants. Bone-graft substitutes: Facts, fictions, and applications. J Bone Joint Surg Am 2001;83-A: 98–103.
3. Wang P, Zhao L, Liu J, Weir MD, Zhou X, Xu HH. Bone tissue engineering via nanostructured calcium phosphate biomaterials and stem cells. Bone Res 2014;2:14017.
4. Marino JT, Ziran BH. Use of solid and cancellous autologous bone graft for fractures and nonunions. Orthop Clin North Am 2010;41:15–26.
5. Kim JH, Kim SM, Kim JH, Kwon KJ, Park YW. Effect of type I collagen on hydroxyapatite and tricalcium phosphate mixtures in rat calvarial bony defects. J Kor Oral Maxillofac Surg 2008;34:36–48.
6. Li J, Baker BA, Mou X, Ren N, Qiu J, Boughton RI, Liu H. Biopolymer/calcium phosphate scaffolds for bone tissue engineering. Adv Healthc Mater 2014;3:469–484.
7. Zou C, Weng W, Deng X, Cheng K, Liu X, Du P, Shen G, Han G. Preparation and characterization of porous beta-tricalcium phosphate/collagen composites with an integrated structure. Biomaterials 2005;26:5276–5284.
8. Arahira T, Todo M. Effects of proliferation and differentiation of mesenchymal stem cells on compressive mechanical behavior of collagen/β-TCP composite scaffold. J Mech Behav Biomed Mater 2014;39:218–230.
9. Wei G, Ma PX. Structure and properties of nano-hydroxyapatite/polymer composite scaffolds for bone tissue engineering. Biomaterials 2004;25:4749–4757.
10. Mickiewicz RA, Mayes AM, Knaack D. Polymer–calcium phosphate cement composites for bone substitutes. J Biomed Mat Res 2002; 61:581–592.
11. Lin HR, Yeh YJ. Porous alginate/hydroxyapatite composite scaffolds for bone tissue engineering: Preparation, characterization, and in vitro studies. J Biomed Mater Res B Appl Biomater 2004; 71:52–65.
12. Lu HH, Kofron MD, El-Amin SF, Attawia MA, Laurencin CT. In vitro bone formation using muscle-derived cells: A new paradigm for bone tissue engineering using polymer-bone morphogenetic protein matrices. Biochem Biophys Res Commun 2003;305:882–889.
13. Azami M, Tavakol S, Samadikuchaksaraei A, Hashjin MS, Baheiraei N, Kamali M, Nourani MR. A porous hydroxyapatite/gelatin nanocomposite scaffold for bone tissue repair: In vitro and in vivo evaluation. J Biomater Sci Polym Ed 2012;23:2353–2368.
14. Baheiraei N, Azami M, Hosseinkhani H. Investigation of magnesium incorporation within gelatin/calcium phosphate nanocomposite scaffold for bone tissue engineering. Int J Appl Ceramic Tech 2015;12:245–253.
15. Hak DJ. The use of osteoconductive bone graft substitutes in orthopaedic trauma. J Am Acad Orthop Surg 2007;15:525–536.
16. Nandi SK, Roy S, Mukherjee P, Kundu B, De DK, Basu D. Orthopaedic applications of bone graft & graft substitutes: A review. Indian J Med Res 2010;132:15–30.
17. LeGeros RZ. Properties of osteoconductive biomaterials: Calcium phosphates. Clin Orthop Relat Res 2002;395:81–98.
18. Klein CP, Driessen AA, de Groot K, van den Hooff A. Biodegradation behavior of various calcium phosphate materials in bone tissue. J Biomed Mater Res 1983;17:769–784.
19. Cameron HU, Macnab I, Pilliar RM. Evaluation of a biodegradable ceramic. J Biomed Mater Res 1977;11:179–186.
20. Nery EB, Lynch KL. Preliminary clinical studies of bioceramic in periodontal osseous defects. J Periodontol 1978;49:523–527.
21. Albee FH. Studies in bone growth: Triple calcium phosphate as a stimulus to osteogenesis. Ann Surg 1920;71:32–39.
22. Komaki H, Tanaka T, Chazono M, Kikuchi T. Repair of segmental bone defects in rabbit tibiae using a complex of beta-tricalcium phosphate, type I collagen, and fibroblast growth factor-2. Biomaterials 2006;27:5118–5126.
23. Ozawa O. Experimental study on bone conductivity and absorbability of the pure β-TCP. J Jpn Soc Biomater 1995;13:167–175.
24. Ohura K, Bohner M, Hardouin P, Lemaître J, Pasquier G, Flautre B. Resorption of, and bone formation from, new beta-tricalcium phosphate-monocalcium phosphate cements: An in vivo study. J Biomed Mater Res 1996;30:193–200.
25. Ohsawa K, Neo M, Matsuoka H, Akiyama H, Ito H, Kohno H, Nakamura T. The expression of bone matrix protein mRNAs around beta-TCP particles implanted into bone. J Biomed Mater Res 2000;52:460–466.
26. Saito M, Shimizu H, Beppu M, Takagi M. The role of beta-tricalcium phosphate in vascularized periosteum. J Ortho Sci 2000;5:275–282.
27. Dong J, Uemura T, Shirasaki Y, Tateishi T. Promotion of bone formation using highly pure porous beta-TCP combined with bone marrow-derived osteoprogenitor cells. Biomaterials 2002;23:4493–4502.
28. Chazono M, Tanaka T, Komaki H, Fujii K. Bone formation and bioresorption after implantation of injectable beta-tricalcium phosphate granules-hyaluronate complex in rabbit bone defects. J Biomed Mater Res A 2004;70:542–549.
29. Ogose A, Hotta T, Hatano H, Kawashima H, Tokunaga K, Endo N, Umezu H. Histological examination of beta-tricalcium phosphate graft in human femur. J Biomed Mater Res 2002;63:601–604.
30. Kondo N, Ogose A, Tokunaga K, Ito T, Arai K, Kudo N, Inoue H, Irie H, Endo N. Bone formation and resorption of highly purified β-tricalcium phosphate in the rat femoral condyle. Biomaterials 2005;26:5600–5608.
31. Al-Munajjed AA, Gleeson JP, O'Brien FJ. Development of a collagen calcium-phosphate scaffold as a novel bone graft substitute. Stud Health Technol Inform 2008;133:11–20.
32. Kamitakahara M, Ohtsuki C, Miyazaki T. Review paper: Behavior of ceramic biomaterials derived from tricalcium phosphate in physiological condition. J Biomater Appl 2008;23:197–212.
33. Best SM, Porter AE, Thian ES, Huang J. Bioceramics: Past, present and for the future. J Eur Cera Soc 2008;28:1319–1327.
34. Koob TJ. Encyclopedia of Biomaterials and Biomedical Engineering. New York: Marcel Dekker; 2004.
35. Bulgin D, Irha E, Hodzic E, Nemec B. Autologous bone marrow derived mononuclear cells combined with β-tricalcium phosphate and absorbable atelocollagen for a treatment of aneurysmal bone cyst of the humerus in child. J Biomater Appl 2013;28:343–353.
36. Zou C, Weng W, Cheng K, Du P, Shen G, Han G, Guan B, Yan W. Porous beta-tricalcium phosphate/collagen composites prepared in an alkaline condition. J Biomed Mater Res A 2008;87:38–44.
37. Guyton GP, Miller SD. Stem cells in bone grafting: Trinity allograft with stem cells and collagen/beta-tricalcium phosphate with concentrated bone marrow aspirate. Foot Ankle Clin 2010;15:611–619.
38. Lu H, Hoshiba T, Kawazoe N, Koda I, Song M, Chen G. Cultured cell-derived extracellular matrix scaffolds for tissue engineering. Biomaterials 2011;32:9658–9666.
39. Pabbruwe MB, Kafienah W, Tarlton JF, Mistry S, Fox DJ, Hollander AP. Repair of meniscal cartilage white zone tears using a stem cell/collagen-scaffold implant. Biomaterials 2010;31:2583–2591.
40. Wang L, Fan H, Zhang ZY, Lou AJ, Pei GX, Jiang S, Mu TW, Qin JJ, Chen SY, Jin D. Osteogenesis and angiogenesis of tissue-engineered bone constructed by prevascularized β-tricalcium

phosphate scaffold and mesenchymal stem cells. Biomaterials 2010;31:9452–9461.
41. Sang L, Luo D, Xu S, Wang X, Li X. Fabrication and evaluation of biomimetic scaffolds by using collagen–alginate fibrillar gels for potential tissue engineering applications. Mater Sci Eng C 2011; 31:262–271.
42. Baheiraei N, Yeganeh H, Ai J, Gharibi R, Azami M, Faghihi F. Synthesis, characterization and antioxidant activity of a novel electroactive and biodegradable polyurethane for cardiac tissue engineering application. Mater Sci Eng C Mater Biol Appl 2014;44: 24–37.
43. Omidvar N, Ganji F, Eslaminejad MB. In vitro osteogenic induction of human marrow-derived mesenchymal stem cells by PCL fibrous scaffolds containing dexamethazone-loaded chitosan microspheres. J Biomed Mater Res A 2016;104:1657–1667.
44. Pouya A, Satarian L, Kiani S, Javan M, Baharvand H. Human induced pluripotent stem cells differentiation into oligodendrocyte progenitors and transplantation in a rat model of optic chiasm demyelination. PLoS One 2011;6:e27925.
45. Semwogerere D, Weeks ER. In: Wnek GE, Bowlin GL, editors. Encyclopedia of Biomaterials and Biomedical Engineering. New York: Marcel Dekker, 2004.
46. León-Mancilla BH, Araiza-Téllez MA, Flores-Flores JO, Piña-Barba MC. Physico-chemical characterization of collagen scaffolds for tissue engineering. J Appl Res Technol 2016;14:77–85.
47. Sarikaya B, Aydin HM. Collagen/beta-tricalcium phosphate based synthetic bone grafts via dehydrothermal processing. BioMed Res Int 2015;2015:1–9.
48. Mann S, Heywood BR, Rajam S, Wade VJ. Molecular recognition in biomineralization. In: Suga S, Nakahara H, editors. Mechanisms and Phylogeny of Mineralization in Biological Systems. Tokyo: Springer-Verlag; 1991. p 47–55.
49. Zhang W, Huang ZL, Liao SS, Cui FZ. Nucleation sites of calcium phosphate crystals during collagen mineralization. J Am Ceram Soc 2003;86:1052–1054.
50. Bigi A, Gandolfi M, Roveri N, Valdré G. In vitro calcified tendon collagen: An atomic force and scanning electron microscopy investigation. Biomaterials 1997;18:657–665.
51. Rhee SH, Lee JD, Tanaka J. Nucleation of hydroxyapatite crystal through chemical interaction with collagen. J Am Ceram Soc 2000;83:2890–2892.
52. Wang Y, Uemura T, Dong J, Kojima H, Tanaka J, Tateishi T. Application of perfusion culture system improves in vitro and in vivo osteogenesis of bone marrow-derived osteoblastic cells in porous ceramic materials. Tissue Eng 2003;9:1205–1214.
53. Novosel EC, Kleinhans C, Kluger PJ. Vascularization is the key challenge in tissue engineering. Adv Drug Deliv Rev 2011;63:300–311.
54. Hegen A, Blois A, Tiron CE, Hellesøy M, Micklem DR, Nör JE, Akslen LA, Lorens JB. Efficient in vivo vascularization of tissue-engineering scaffolds. J Tissue Eng Regen Med 2011;5:e52–e62.